

## Original Article



## OPEN ACCESS

**Received:** May 23, 2023  
**Revised:** Jul 29, 2023  
**Accepted:** Aug 8, 2023  
**Published online:** Sep 6, 2023

### Correspondence to

#### Nagaraj Manickam

Department of Vascular Biology, Madras  
Diabetes Research Foundation, No. 4, Conran  
Smith Road, Gopalapuram, Chennai 600 086,  
India.  
Email: nagaraj@mdrf.in

Copyright © 2023 The Korean Society of Lipid  
and Atherosclerosis.

This is an Open Access article distributed  
under the terms of the Creative Commons  
Attribution Non-Commercial License ([https://  
creativecommons.org/licenses/by-nc/4.0/](https://creativecommons.org/licenses/by-nc/4.0/))  
which permits unrestricted non-commercial  
use, distribution, and reproduction in any  
medium, provided the original work is properly  
cited.

### ORCID iDs

Saravanakumar Sundararajan   
<https://orcid.org/0009-0004-9572-2950>  
Isaivani Jayachandran   
<https://orcid.org/0009-0005-4595-3141>  
Gautam Kumar Pandey   
<https://orcid.org/0000-0003-0140-718X>  
Saravanakumar Venkatesan   
<https://orcid.org/0009-0003-5759-4217>  
Anusha Rajagopal   
<https://orcid.org/0009-0001-2723-518X>  
Kuppan Gokulakrishnan   
<https://orcid.org/0000-0003-3167-8239>  
Muthuswamy Balasubramanyam   
<https://orcid.org/0000-0001-9013-7024>  
Viswanathan Mohan   
<https://orcid.org/0000-0001-5038-6210>

# Metformin Reduces the Progression of Atherogenesis by Regulating the Sestrin2-mTOR Pathway in Obese and Diabetic Rats

Saravanakumar Sundararajan <sup>1</sup>, Isaivani Jayachandran <sup>1,2</sup>,  
Gautam Kumar Pandey <sup>1</sup>, Saravanakumar Venkatesan <sup>1</sup>, Anusha Rajagopal <sup>1</sup>,  
Kuppan Gokulakrishnan <sup>3</sup>, Muthuswamy Balasubramanyam <sup>4</sup>,  
Viswanathan Mohan <sup>5</sup>, Nagaraj Manickam <sup>1</sup>

<sup>1</sup>Department of Vascular Biology, Madras Diabetes Research Foundation & ICMR Centre for Advanced Research on Diabetes, Chennai, India

<sup>2</sup>Department of Biotechnology, Sri Venkateswara College of Engineering, Sriperumbudur, India

<sup>3</sup>Department of Neurochemistry, National Institute of Mental Health and Neurosciences (NIMHANS), Hosur Road, Bengaluru, India

<sup>4</sup>Department of Cell and Molecular Biology, Madras Diabetes Research Foundation & ICMR Centre for Advanced Research on Diabetes, Chennai, India

<sup>5</sup>Madras Diabetes Research Foundation and Dr. Mohan's Diabetes Specialities Centre, Chennai, India

## ABSTRACT

**Objective:** In previous research, we found that Sestrin2 has a strong association with plasma atherogenicity and combats the progression of atherogenesis by regulating the AMPK-mTOR pathway. Metformin, an activator of AMPK, is widely used as a first-line therapy for diabetes, but its role in preventing atherosclerosis and cardiac outcomes is unclear. Hence, we aimed to assess the effect of metformin on preventing atherosclerosis and its regulatory role in the Sestrin2-AMPK-mTOR pathway in obese/diabetic rats.

**Methods:** Animals were fed a high-fat diet to induce obesity, administered streptozotocin to induce diabetes, and then treated with metformin (150 mg/kg body weight) for 14 weeks. Aorta and heart tissues were analyzed for Sestrin2 status by western blotting and immunohistochemistry, AMPK and mTOR activities were investigated using western blotting, and atherogenicity-related events were evaluated using reverse transcription quantitative polymerase chain reaction and histology.

**Results:** Obese and diabetic rats showed significant decrease in Sestrin2 levels and AMPK activity, accompanied by increased mTOR activity in the heart and aorta tissues. Metformin treatment significantly restored Sestrin2 and AMPK levels, reduced mTOR activity, and restored the altered expression of inflammatory markers and adhesion molecules in obese and diabetic rats to normal levels. A histological analysis of samples from obese and diabetic rats showed atherosclerotic lesions both in aorta and heart tissues. The metformin-treated rats showed a decrease in atherosclerotic lesions, cardiac hypertrophy, and cardiomyocyte degeneration.

**Conclusion:** This study presents further insights into the beneficial effects of metformin and its protective role against atherosclerosis through regulation of the Sestrin2-AMPK-mTOR pathway.

**Keywords:** Metformin; Diabetes mellitus; Obesity; Atherosclerosis; Sestrin2

Nagaraj Manickam <https://orcid.org/0000-0002-0049-777X>**Funding**

The study is supported by a research grant from MDRF intramural funding.

**Conflict of Interest**

The authors have no conflicts of interest to declare.

**Data Availability Statement**

The datasets generated during and/or analyzed during the current study are available from the corresponding author on reasonable request.

**Author Contributions**

Conceptualization: Sundararajan S, Manickam N; Formal analysis: Gokulakrishnan K, Manickam N; Funding acquisition: Manickam N; Investigation: Sundararajan S; Methodology: Sundararajan S, Jayachandran I, Pandey G, Venkatesan S, Rajagopal A; Project administration: Manickam N; Supervision: Balasubramanyam M, Manickam N; Validation: Manickam N; Writing - original draft: Sundararajan S, Jayachandran I, Manickam N; Writing - review & editing: Sundararajan S, Jayachandran I, Venkatesan S, Rajagopal A, Gokulakrishnan K, Balasubramanyam M, Mohan V, Manickam N.

## INTRODUCTION

Metabolic syndrome is a cluster of various metabolic disorders, including obesity and prediabetes or type 2 diabetes, and it is closely associated with cardiovascular disease (CVD).<sup>1,2</sup> According to the World Health Organization, more than 1.9 billion adults on the earth are overweight (body mass index [BMI] >25 kg/m<sup>2</sup>), out of whom 650 million people are obese (BMI >30 kg/m<sup>2</sup>).<sup>3</sup> CVD is a disorder affecting the heart and blood vessels (arteries), resulting from atherosclerosis, which develops from the build-up of plaque inside the arteries. The resultant narrowing and hardening of the artery walls make it harder for blood to flow.<sup>4</sup>

The process of atherogenic progression begins with endothelial injury, followed by the activation of monocytes towards the M1 phenotype. These activated monocytes migrate into the endothelium, a process facilitated by adhesion molecules such as intercellular adhesion molecule-1 (ICAM-1) and vascular cell adhesion molecule-1 (VCAM-1). Once inside the endothelium, they differentiate into macrophages, which ingest atherogenic lipoproteins and transform into lipid-laden foam cells.<sup>5</sup> In previous research, we discovered that Sestrin2 helps to combat the progression of atherogenesis by regulating the AMPK-mTORC1 pathway, which plays a significant role in monocyte activation.<sup>6</sup> Additionally, we found a correlation between decreased levels of Sestrin2 and increased plasma atherogenicity in patients with diabetes and dyslipidemia.<sup>7</sup>

Metformin, a well-known biguanide class drug and an AMPK activator, has been extensively used as a first-line treatment for type 2 diabetes mellitus over the past 50 years. A previous study demonstrated that metformin significantly reduced the progression of carotid artery intima-media thickness, a recognized indicator of atherosclerotic progression, in patients with diabetes.<sup>8</sup> Beyond its primary role in insulin sensitization, metformin also regulates the AMPK-mTORC1 pathway and inhibits both monocyte activation and the secretion of pro-inflammatory cytokines.<sup>9</sup>

However, the role of metformin in regulating the Sestrin-mTOR nexus via the AMPK pathway, particularly in relation to the progression of atherosclerosis and cardiac hypertrophy, remains unclear. Therefore, our study was designed to evaluate the role of metformin in modulating the Sestrin2-mTOR pathway, monocyte activation, and atherogenic events in a preclinical obese/diabetic animal model.

## MATERIALS AND METHODS

### 1. Animal model: experimental design

Male Wistar rats (4–5 weeks of age, purchased from the National Institute of Nutrition, Hyderabad, India) were randomly assigned to 5 groups (n=6 in each group). The groups were categorised based on body weight and blood glucose levels as follows: 1) control (normal pellet diet, NPD), 2) obese (high-fat diet, HFD), 3) obese + metformin (HFD+MET), 4) diabetes (HFD + STZ), 5) diabetes + MET (HFD + STZ + MET). The experimental design is detailed in **Supplementary Fig. 1**. Rats in the HFD group were fed a HFD, with 65% of calories derived from fat. The control group was given a NPD, sourced from NIN, Hyderabad, India. Obesity was confirmed by analysing body weight and lipid profile. Insulin resistance was verified through an insulin tolerance test (ITT), as described elsewhere.<sup>10</sup> Diabetes was induced by partially damaging the pancreas with a single intraperitoneal injection of

streptozotocin (STZ) (Sigma-Aldrich, MO, USA) at a dose of 25 mg/kg body weight. For the non-diabetic groups, a citrate buffer was administered instead. An oral glucose tolerance test (OGTT)<sup>10</sup> was performed 5 days after the administration of STZ. The animals were considered to have diabetes if their blood glucose level increased to  $\geq 15$  mmol/L (270 mg/dL). Upon confirmation of diabetes onset, MET (Glenmark Pharmaceuticals, Mumbai, India) was orally administered to the respective groups at a dose of 150 mg/kg body weight. After 14 weeks of MET treatment, fasting blood samples were collected for biochemical assays. The rats were then euthanised, and heart and aorta tissues were excised and stored at  $-80^{\circ}\text{C}$ . For histological studies, the tissues were preserved in 10% formalin. All experimental procedures adhered to the National Institutes of Health guide for the care and use of laboratory animals (NIH Publications No. 8023, revised 1978), as well as the guidelines of the Committee for Control and Supervision on Experiments on Animals (CPCSEA), Government of India. The study was approved by the Institutional Animal Ethics Committee (IAEC) of the Madras Diabetes Research Foundation, Chennai, India.

## 2. Biochemical measurements

Fasting plasma glucose (hexokinase method), serum cholesterol (cholesterol oxidase-peroxidase-amidopyrine method), serum triglycerides (glycerol phosphate oxidase-peroxidase-amidopyrine method), and high-density lipoprotein (HDL) cholesterol (direct method-polyethylene glycol pre-treated enzymes) were measured using a Hitachi-912 Autoanalyzer (Hitachi, Mannheim, Germany).

## 3. Total RNA isolation from tissues and real-time polymerase chain reaction

The tissues were thoroughly homogenised using a bullet blender (Next Advance, Inc., Troy, NY, USA). We isolated total RNA from the aorta and heart using the conventional method with the TRIzol reagent (Sigma, St. Louis, MO, USA), as outlined in other sources. We utilised real-time polymerase chain reaction analysis to examine the expression of targeted genes, following the methodology detailed in our previous study.<sup>6</sup> The gene primer sequences are given in **Supplementary Table 1**.

## 4. Immunoblotting

The tissue homogenate was centrifuged at  $15,000 \times g$  at  $4^{\circ}\text{C}$ , after which the supernatant was separated from the tissue debris. The protein concentrations of tissue homogenates were determined using Bradford reagents (Bio-Rad, Hercules, CA, USA). These were then probed for Sestrin2 (#10795-1-AP; Proteintech, Rosemont, IL, USA), pAMPK (Thr172, #2531), AMPK (#2532), mTOR (#2972), pmTOR (Ser2448, #2971; Cell Signaling Technology, Danvers, MA, USA), and  $\beta$ -actin (#SC-81178; Santa Cruz Biotechnology, Dallas, TX, USA) through immunoblotting, as described in our previous study.<sup>6</sup> The protein bands were made visible using an enhanced chemiluminescent reagent (Bio-Rad) and a Bio-Rad gel-doc instrument. The intensity of these bands was quantified using ImageJ software (NIH, Bethesda, MD, USA).

## 5. Immunohistochemistry

Formalin-fixed aorta and heart tissues were sliced into 3-mm sections on charged slides, deparaffinised, and rehydrated. The slides were then incubated with a Sestrin2 (CST, Danvers, MA, USA) antibody for 30 minutes in a moist chamber and then washed twice with wash buffer. The slides were first incubated with PolyExcel target binder reagent, and then with PolyExcel HRP followed by the DAB chromogen for 5 minutes, and then washed with distilled water. Finally, the slides were incubated with counterstain haematoxylin for 30 seconds and then washed with distilled water. After that, the slides were allowed to dehydrate

and then mounted using mounting media. Protein expression was observed under a light microscope.

### 6. Histopathology

The heart and aorta tissue samples were washed with normal saline to remove the blood cells and fixed in 10% buffered formaldehyde solution. The samples were then embedded in paraffin wax, subjected to automatic tissue processing, and 5- $\mu$ m sections were prepared. These sections were stained with haematoxylin and eosin for general histopathology. After that, the histopathological profile of each sample was observed under a light microscope.

### 7. Statistical analysis

GraphPad Prism Version 5 was used for statistical analysis. Multiple comparisons were done by one-way analysis of variance (ANOVA), followed by a post-hoc analysis using the Tukey test. All values are represented as mean  $\pm$  SEM, and  $p$ -values  $<0.05$  were considered statistically significant.

## RESULTS

### 1. Confirmation of obesity and insulin resistance in HFD-fed Wistar rats

To confirm obesity, we analysed changes in body weight and plasma lipid profiles in animals after 45 days of HFD feeding. The HFD animals exhibited a significant increase in body weight and notable alterations in lipid profiles, as depicted in **Supplementary Fig. 2**. The ITT revealed that the HFD-fed rats had a reduced glucose disposal in the blood following insulin administration, compared to the control rats (**Supplementary Fig. 3A**). Additionally, the area under the curve (AUC) for the glucose disposal curve was significantly higher in the HFD group (6,077 $\pm$ 326.5) than in the NPD group (4,318 $\pm$ 264.0) ( $p<0.05$ ), as shown in **Supplementary Fig. 3B**. These findings suggest that rats fed an HFD became both obese and insulin-resistant.

### 2. Confirmation of diabetes in the HFD fed and low-dose STZ-administered rats

To confirm the onset of diabetes in rats treated with HFD + STZ, we performed an OGTT. These rats showed significantly elevated glucose levels at all measured time points (0, 30, 60, and 120 minutes) compared to the control and HFD groups (**Supplementary Fig. 3C**). Additionally, the AUCs of blood glucose concentration following the glucose challenge in the STZ-treated, HFD-fed group (1,029 $\pm$ 57.81) were significantly higher than those in the control (332.0 $\pm$ 9.369) and HFD-fed alone (373.5 $\pm$ 6.891) groups ( $p<0.05$ ) (**Supplementary Fig. 3D**). However, no significant difference was observed between the control and HFD-fed groups. This suggests that the animals fed only HFD became insulin resistant but did not develop diabetes, while the animals treated with a low dose of STZ and fed with HFD developed both insulin resistance and diabetes. Therefore, we divided the groups into obese (HFD) and diabetic (HFD+STZ) animals.

### 3. Clinical and biochemical characteristics of experimental rats

The obese and diabetic rats exhibited higher levels of cholesterol ( $p<0.001$ ), triglycerides ( $p<0.05$ ), very-low-density lipoprotein cholesterol (VLDL-C) ( $p<0.05$ ), and the total cholesterol to HDL-C (CHO/HDL-C) ratio ( $p<0.05$ ) compared to the control rats. The fasting plasma glucose in diabetic rats was four times greater than that in the control animals ( $p<0.001$ ). Additionally, the plasma atherogenic index value, a logarithmically transformed

ratio of molar concentrations of triglycerides to HDL-cholesterol that predicts cardiovascular risk, was significantly higher in obese and diabetic rats than in control rats. The elevated fasting plasma glucose, cholesterol, triglycerides, VLDL-C, CHO/HDL-C values, and plasma atherogenic index were significantly lower in the MET treatment group (HFD + STZ + MET) than in the diabetic group ( $p < 0.05$ ). The elevated VLDL-C also significantly decreased in MET-treated obese rats (HFD + MET) compared to control rats. Obese animals demonstrated a significant increase in body weight, but no significant difference was observed between the control and diabetic rat groups. There was also a moderate increase in the weight of the aorta in diabetic rats compared to the control group. The MET-treated rats (HFD + STZ + MET) exhibited reduced heart weight compared to the diabetic rats (**Supplementary Table 2**).

#### **4. Effect of MET on mRNA expression of Sestrin2 in aorta and heart of obese and diabetic rats**

In our previous study, we noted a significant decrease in the level of Sestrin2 in both monocytes and the circulation of patients with diabetes and dyslipidaemia.<sup>7</sup> Hence, we aimed to analyse the status of Sestrin2 expression in the aorta and heart tissues of obese and diabetic rats.

The mRNA expression of Sestrin2 was notably diminished in the aortas of obese rats. However, the group treated with MET exhibited a significant increase in comparison to both the control and HFD groups (**Fig. 1A**). Despite this, no significant difference was observed in Sestrin2 expression in the heart between the NPD and HFD groups, as depicted in **Fig. 1A**.

In the diabetic model, we observed a significant decrease in the expression of Sestrin2 in both the aorta and heart, compared to control rats. The group treated with MET (HFD + STZ + MET) exhibited a significant increase in Sestrin2 expressions compared to the diabetic group (**Fig. 1B**). These findings confirm a significant reduction in Sestrin2 expression in heart and aorta tissues under obese and diabetic conditions, and MET treatment effectively restored Sestrin2 expression.

#### **5. Immunohistochemistry assessment of Sestrin2 expression in the aorta and heart of obese and diabetic rats**

We subsequently conducted an immunohistochemical analysis to localize the Sestrin2 expression in the aorta and heart. Obese rats exhibited a reduced expression of Sestrin2 in the tunica adventitia of the aorta. In contrast, the group treated with MET demonstrated an increased expression of Sestrin2 in both the tunica adventitia and tunica media of the aorta (**Fig. 1C**). Similarly, in the heart, we noted decreased expression of Sestrin2 in HFD rats, while in control rats, we detected mild, multifocal expression of Sestrin2 in the cytoplasm of myocytes. The group treated with MET exhibited higher expression of Sestrin2 in myocytes than the HFD rats (**Fig. 1D**).

The diabetic rats showed decreased or meagre expression of Sestrin2 in the tunica adventitia of the aorta, as well as a decreased or scant expression of Sestrin2 in the degenerated myocytes of the heart (**Fig. 1C and D**). The group treated with MET (HFD + STZ + MET) demonstrated a restoration of Sestrin2 expression in both the tunica adventitia and tunica media of the aorta. Additionally, there was an increased multifocal expression of Sestrin2 in the heart's myocytes compared to the control and diabetic rats (**Fig. 1C and D**). This underscores the role of MET in restoring Sestrin2 expression in both aorta and heart tissues.

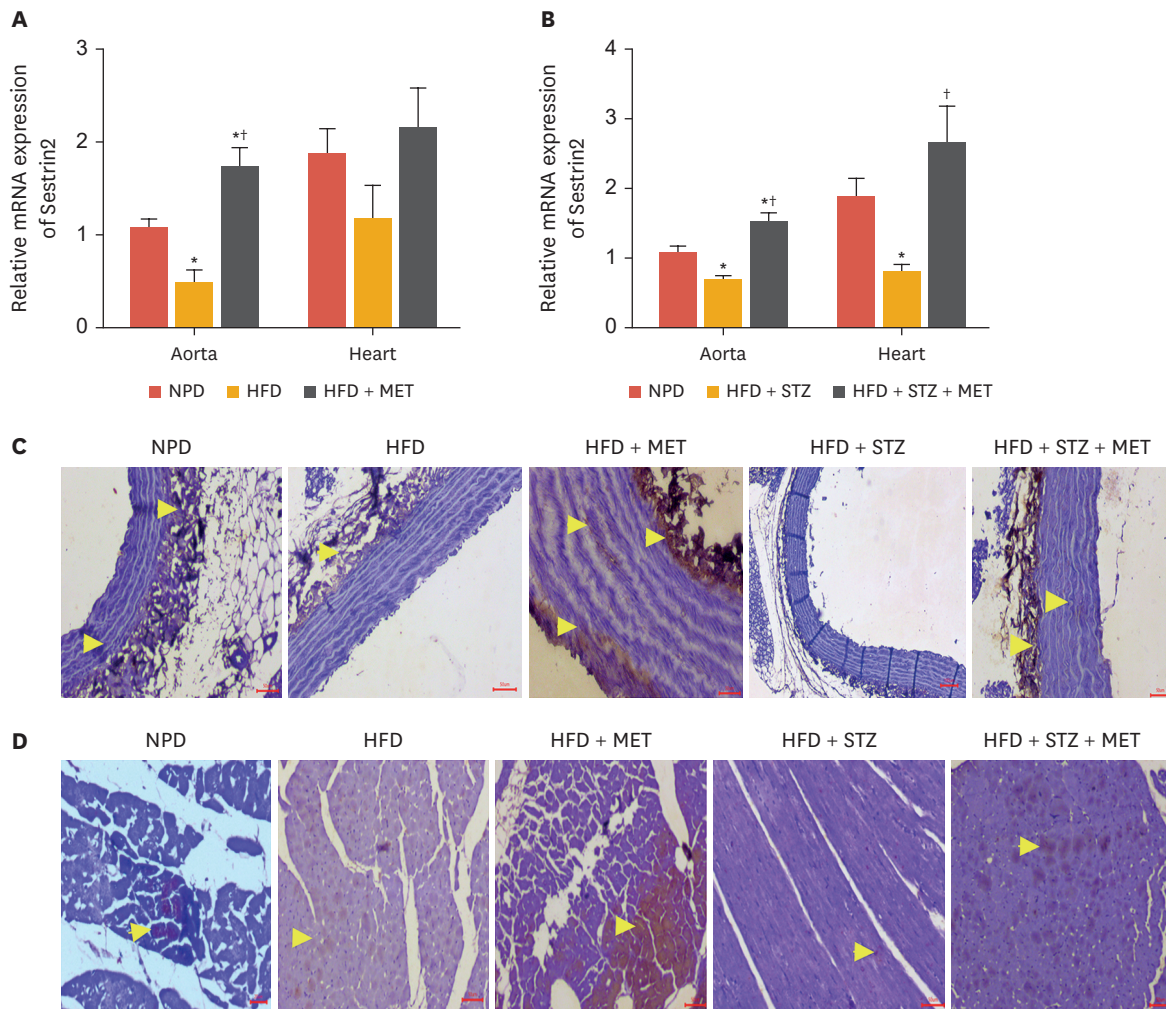


**Fig. 1.** Effect of metformin on mRNA expression of Sestrin2. (A, B) Relative mRNA expression of Sestrin2 in the aorta and heart of obese and diabetes rats. (C, D) Representative images of the immunohistochemistry of Sestrin2 expression in thoracic aorta and heart tissues (yellow arrow) ( $\times 10$ , bar=50  $\mu\text{m}$ ). All values are represented as mean  $\pm$  SEM.

NPD, normal-pellet diet; HFD, high-fat diet; MET, metformin; STZ, streptozotocin.

\* $p < 0.05$  compared with NPD, † $p < 0.05$  compared to HFD/HFD + STZ.

## 6. Role of MET in the regulation of Sestrin2-AMPK-mTOR nexus in aorta and heart of obese and diabetic rats

We observed a significant decrease in Sestrin2 expression and AMPK activation, along with a significant rise in mTORC1 activation, in both the aorta and heart of obese and diabetic rats compared to control rats. In contrast, the groups treated with MET demonstrated a significant increase in Sestrin2 and AMPK activation, and a significant decrease in mTOR activation (**Fig. 2A-D**). These findings suggest that MET may play a role in regulating the Sestrin2-mTOR pathway.

## 7. Effect of MET on the status of pro-inflammatory (M1) and anti-inflammatory (M2) markers in aorta and heart of obese and diabetic rats

Since inflammation plays a significant role in atherogenesis, we investigated the impact of MET on the status of pro-inflammatory (M1) and anti-inflammatory (M2) markers in aorta and heart tissues. We observed a significant increase in the mRNA expressions of iNOS and tumor necrosis factor (TNF)- $\alpha$  (M1 markers), and a significant decrease in the mRNA

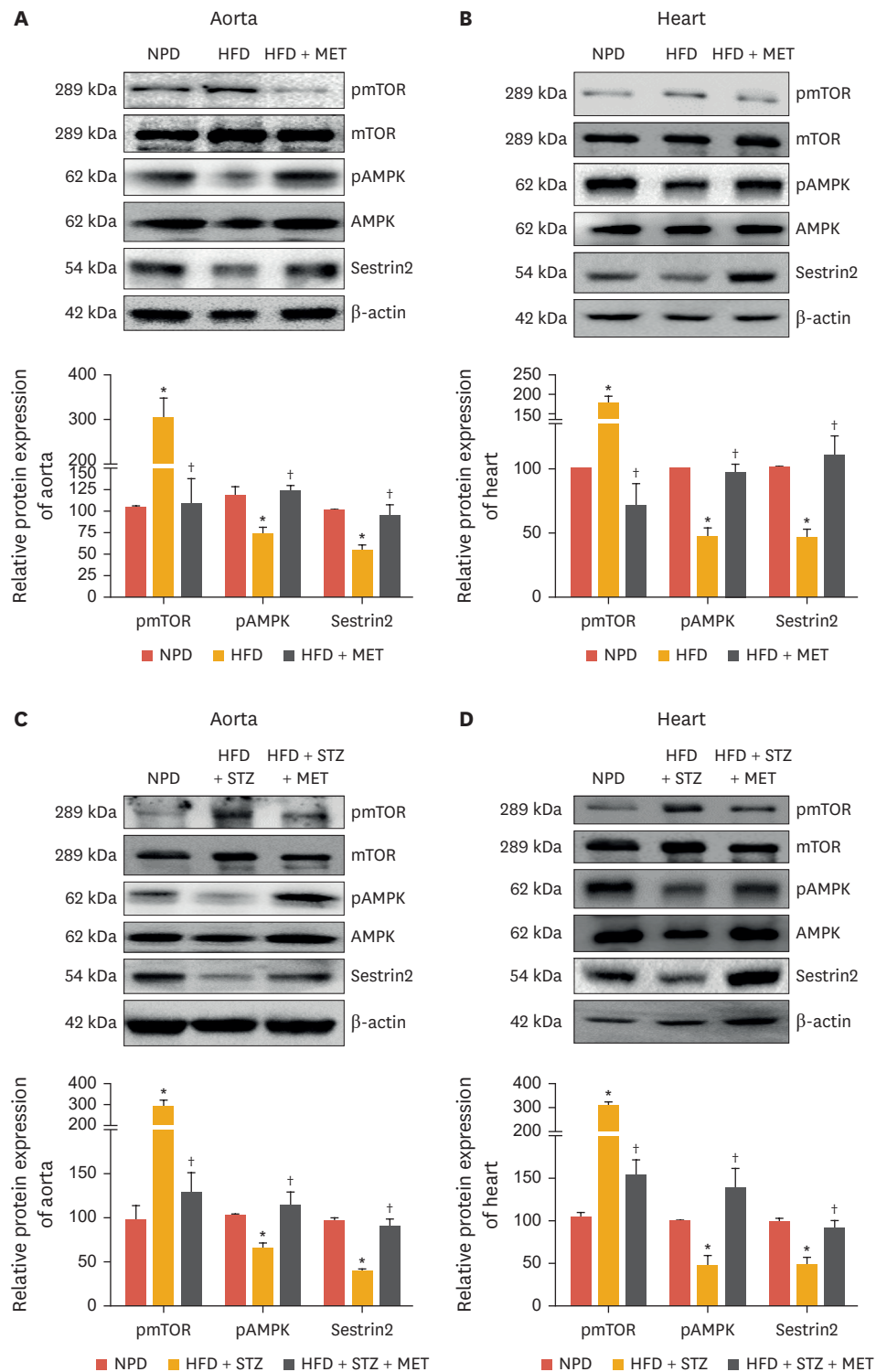


**Fig. 2.** Effect of metformin on Sestrin2-mTOR. (A, B, C, D) Protein expression and cumulative bar graph of Sestrin2, pmTOR (Ser2448), mTOR, pAMPK (Thr172), AMPK and  $\beta$ -actin. All values are represented as mean  $\pm$  SEM. NPD, normal-pellet diet; HFD, high-fat diet; MET, metformin; STZ, streptozotocin. \* $p < 0.05$  compared with NPD, † $p < 0.05$  compared to HFD/HFD + STZ.

expressions of Arg-1 and transforming growth factor (TGF)- $\beta$  (M2 markers) in the aorta of obese animals compared to the control group (**Fig. 3A and B**). Similarly, in the heart, the obese group exhibited a significant increase in TNF- $\alpha$  (M1) and a significant decrease in ARG-1 (M2) compared to the control group, as depicted in **Fig. 3C and D**. Treatment with MET normalized the abnormal levels of M1 and M2 markers in obese rats (**Fig. 3A-D**).

In the diabetic model, we observed a significant increase in the mRNA expressions of iNOS and TNF- $\alpha$ , along with a significant decrease in the mRNA expressions of Arg-1 and TGF- $\beta$ , when compared to the aorta and heart from the control group, as depicted in **Fig. 3E-H**. Rats treated with MET (HFD + STZ + MET) demonstrated a significant reduction in the M1 markers and a significant elevation in the M2 markers, relative to the diabetic group (**Fig. 3E-H**). These findings suggest that MET treatment effectively counters pro-inflammatory tendencies (M1) in the aorta and heart of obese and diabetic rats.

### **8. Effect of MET on adhesion molecules in aorta and heart of obese and diabetic rats**

Monocyte adhesion to endothelial cells is another key event in the progression of atherosclerosis. Therefore, we examined the expression of adhesion molecules such as CCL-2, ICAM-1, and VCAM-1 in the aorta and heart tissues. We found a significant increase in the expression of VCAM-1 (**Fig. 4A**) in the aorta, and a significant increase in the expressions of CCL-2 and ICAM-1 (**Fig. 4B**) in the hearts of obese rats compared to the control group. However, there was no significant difference observed in the gene expression of adhesion molecules with MET treatment in both the aorta and heart when compared to obese animals, as shown in **Fig. 4A and B**.

In the diabetic model, there was a significant increase in the mRNA expressions of CCL-2, ICAM-1, and VCAM-1 in both the aorta and heart of HFD + STZ rats, compared to control rats, as depicted in **Fig. 4C and D**. Treatment with MET (HFD + MET + STZ) significantly reduced the expression of CCL-2, ICAM-1, and VCAM-1 in the heart, but no significant difference was observed in the aorta when compared to diabetic animals, as shown in **Fig. 4C and D**. These results suggest that MET treatment significantly impacts adhesion molecules in the heart, which aids in preventing the infiltration of mononuclear cells (MNCs).

### **9. Role of MET on matrix metalloproteinases in the aorta and heart of obese and diabetic rats**

Next, we examined the expression levels of matrix metalloproteinase molecules (MMP2 and MMP9), as well as the regulator of these enzymes (TIMP-1), in rat tissues (aorta and heart). We found that the mRNA expression of MMP2 and MMP9 was significantly elevated in the obese and diabetic groups compared to the NPD group in both the aorta and heart. The groups treated with MET (HFD + MET & HFD + STZ + MET) exhibited lower levels of MMP2 and MMP9 expression than in the pathological groups, as shown in **Fig. 4E-H**. The MET-treated group (HFD + MET) demonstrated an increased expression of TIMP-1 in the hearts of obese rats (**Fig. 4F**), while the decreased TIMP-1 expression in the aorta of the diabetic group was augmented by MET treatment (HFD + STZ + MET) (**Fig. 4G**). These findings suggest that MET may decrease the expression of matrix metalloproteinases.



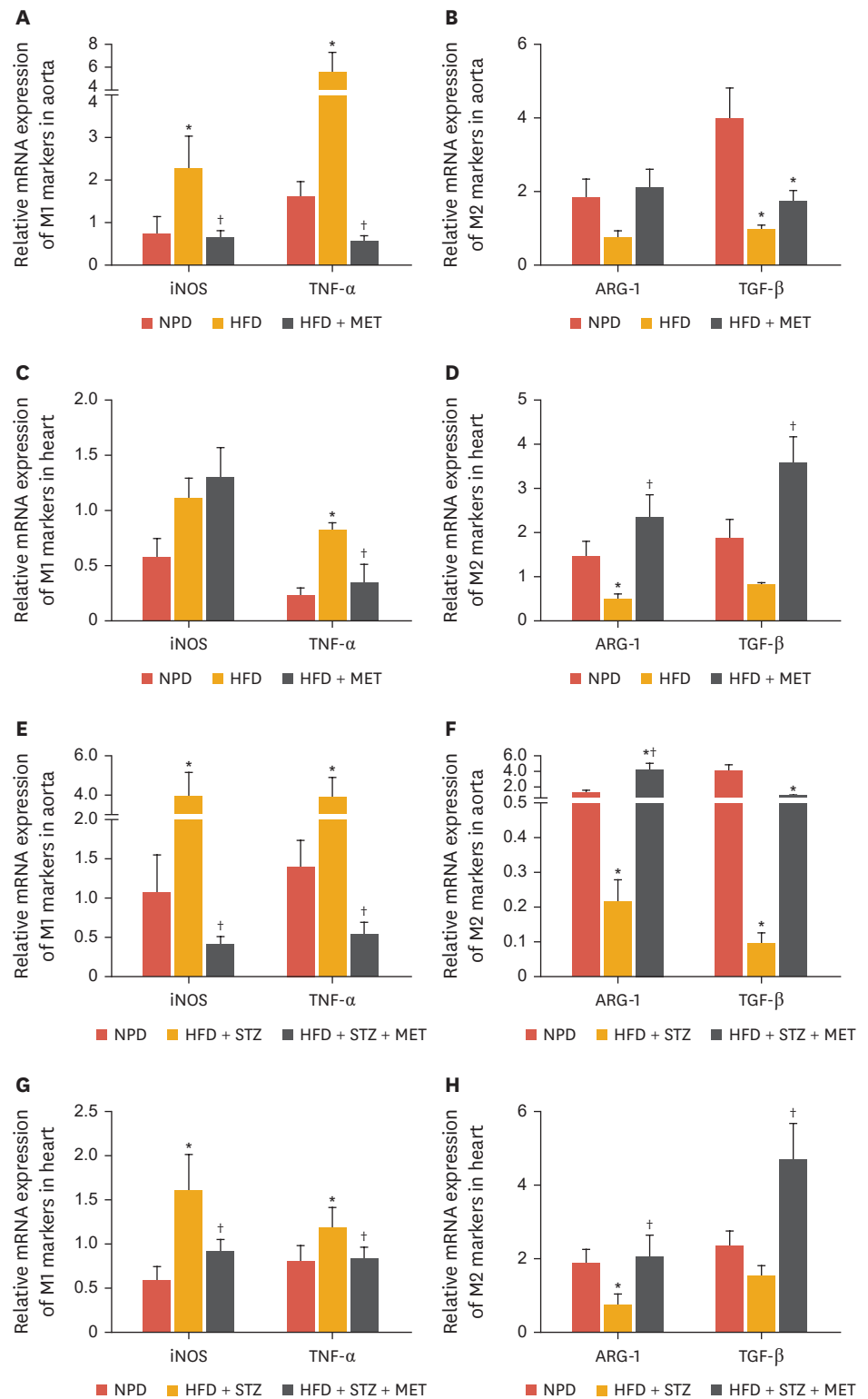


**Fig. 3.** Role of metformin on the status M1 and M2 markers. (A, C, E, G) Relative mRNA expression of iNOS, TNF- $\alpha$  (M1 markers) in the aorta and heart of obese and diabetes rats. (B, D, E, G) Relative mRNA expression of ARG-1, TGF- $\beta$  (M2 markers) in the aorta and heart of obese and diabetes rats. All values are represented as mean  $\pm$  SEM. TNF, tumor necrosis factor; NP, normal-pellet diet; HD, high-fat diet; M, metformin; TGF, transforming growth factor; STZ, streptozotocin. \* $p < 0.05$  compared with NP, † $p < 0.05$  compared with HD/HD + STZ.

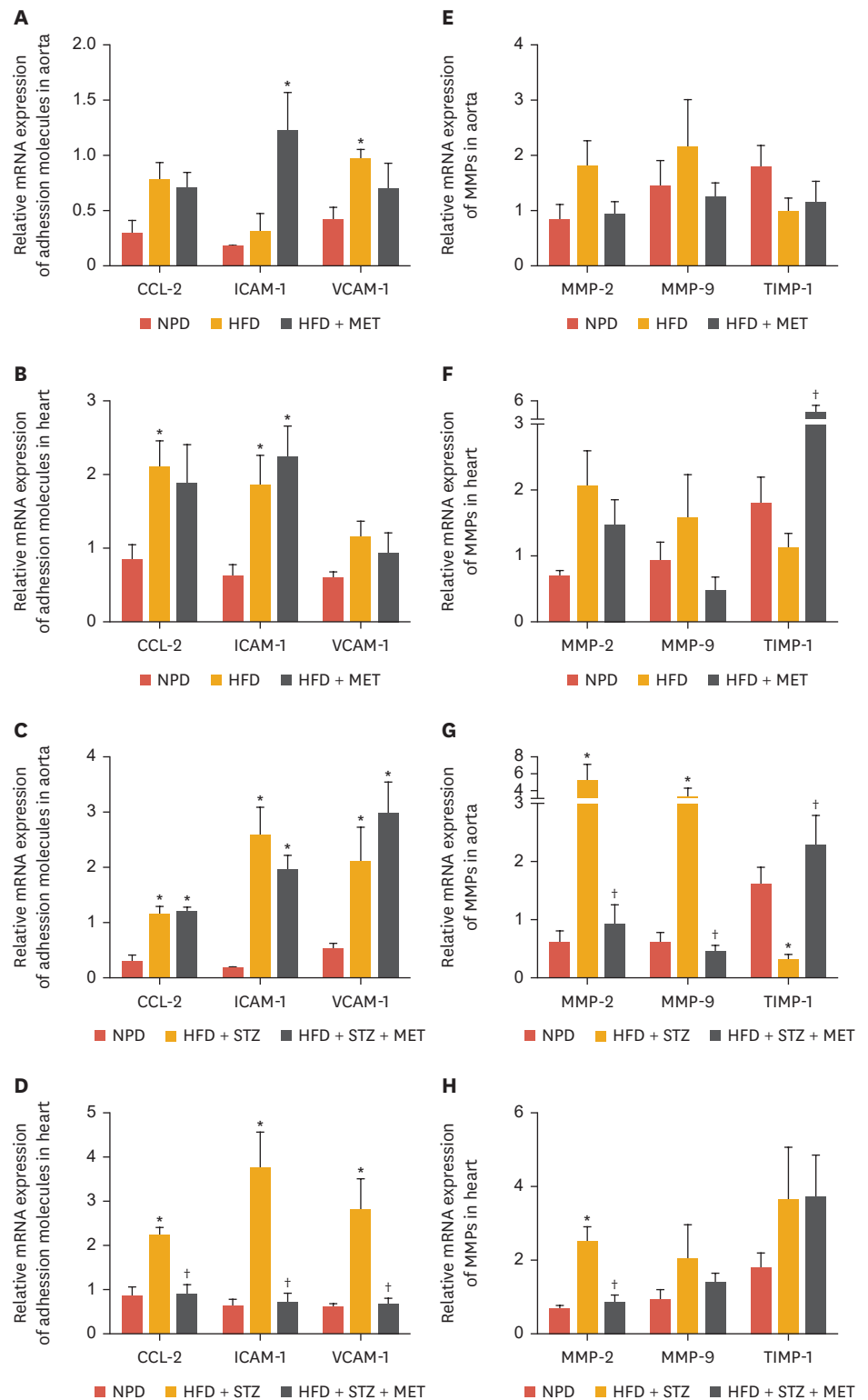


**Fig. 4.** Role of metformin on the expression of adhesion molecules and MMPases. (A, B, C, D) Relative mRNA expression of CCL2, ICAM-1, VCAM-1 (adhesion molecules) in aorta and heart of obese and diabetes rats. E, F, G, H) Relative mRNA expression of MMP2, MMP9 (MMPases) and TIMP-1 (regulator of MMPases) in the aorta of obese and diabetes rats. All values are represented as mean  $\pm$  SEM. NPD, normal-pellet diet; HFD, high-fat diet; MET, metformin; STZ, streptozotocin; MMP, matrix metalloprotein. \* $p < 0.05$  compared with NPD, † $p < 0.05$  compared to HFD/HFD + STZ.

**10. Histopathological assessment of aorta on the effect of MET in the progression of atherogenesis of obese and diabetic rats**

**Fig. 5** depicts the histology of the aorta in experimental rats. In the aortas of obese rats, there was an observed increase in thickness and disorganization of fibers, fragmentation, and the presence of vacuoles in the tunica media, indicative of atherosclerotic lesions (**Fig. 5B**).

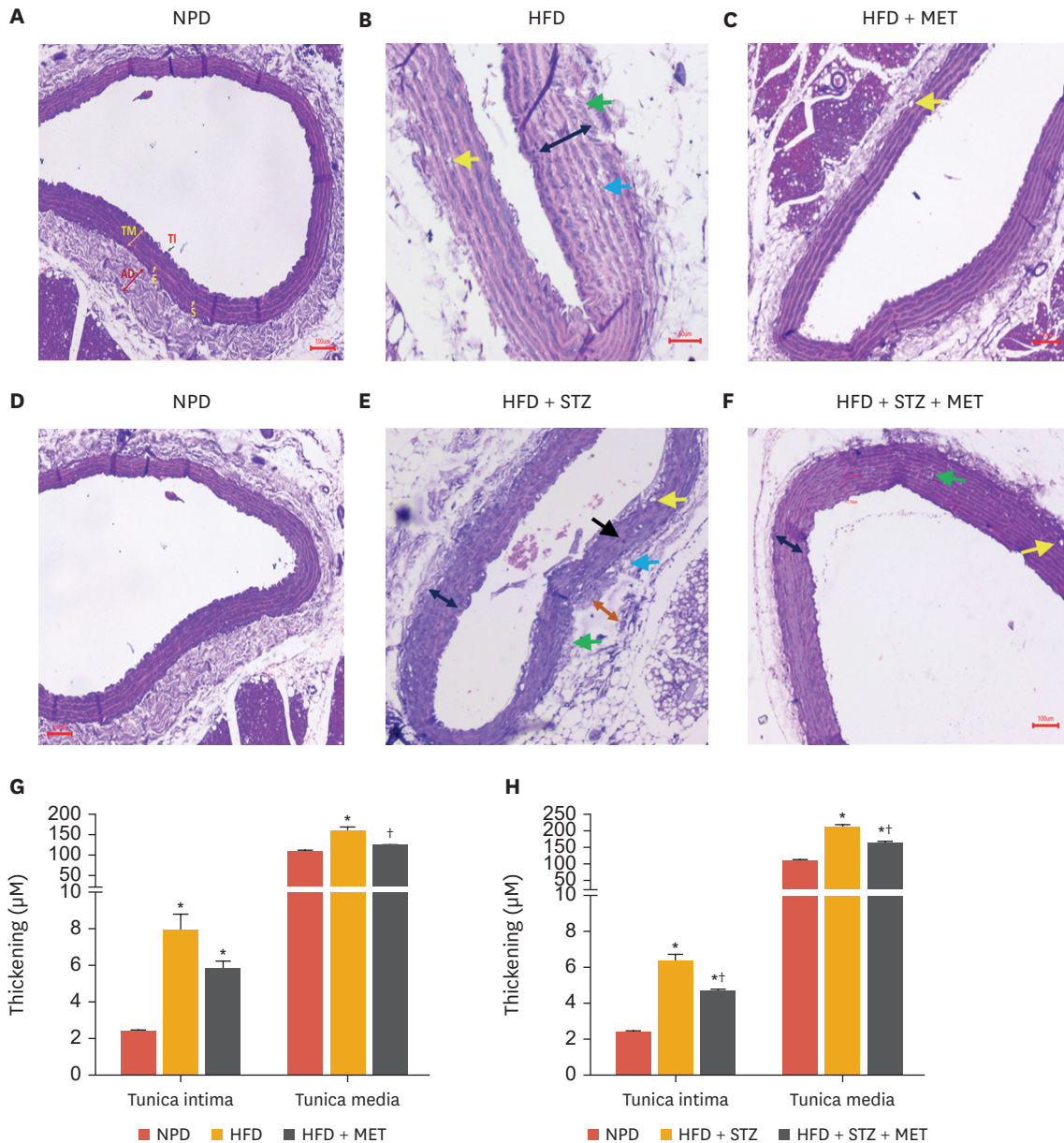


**Fig. 5.** Transverse sections of aorta of rats. (A, D) NP rats show the normal histological structure of thin smooth tunica intima, regularly arranged parallel elastic laminae (E) of the tunica media with regularly arranged spindle smooth muscle fibers (S) between the tunica media and adventitia (AD) which is formed from loose connective tissue. (B) HFD rats show a thickening of tunica media (dark blue color two-way arrow), vacuolation (yellow arrow), disorganization of fibers (green arrow), degeneration of smooth muscle fibers (light blue arrow) in tunica media. (C) HFD+MET rats show decreased disorganization of fibers, decreased fragmentation and vacuoles in tunica media. (E) HFD+STZ rats show thickening of the tunica media, disorganization of fibers, fragmentation of smooth muscle fibers in tunica media, vacuolation, mononuclear cell infiltrations (black arrow) and separation of tunica media from adventitia (brown color two-way arrow). (F) HFD+STZ+MET rats show decreased disorganization of fibers, decreased fragmentation and vacuoles in tunica media. (G, H) Measurement of tunica intima and media thickness (mean ± SEM). (Histological structure analysis using haematoxylin and eosin staining, scale bar: ×4=100 µm). NP, normal-pellet diet; HFD, high-fat diet; MET, metformin; STZ, streptozotocin. \**p*<0.05 compared with NP, †*p*<0.05 compared to HFD/HFD + STZ.

Treatment with MET demonstrated a reduction in fiber disorganization, fragmentation, and vacuoles in the tunica media (**Fig. 5C**).

We observed increased thickness and severe fragmentation in the tunica media of diabetic rats, along with disorganization of fibers. We also observed numerous vacuoles and MNC infiltration in both the tunica media and tunica intima, as well as a separation of the tunica media from the adventitia in these diabetic rats (**Fig. 5E**). In contrast, the group treated with MET (HFD + STZ + MET) exhibited only mild or reduced disorganization of fibers and a few vacuoles in the tunica media (**Fig. 5F**).

We measured the thickness of the tunica media and tunica intima and found a significant increase in the obese group compared to the control group. MET treatment notably reduced the thickness of the tunica media in comparison to the HFD rats, as depicted in **Fig. 5G**. Similarly, the thickness of the tunica media and tunica intima was significantly higher in the diabetic group compared to the control group. MET treatment (HFD + STZ + MET) significantly reduced the thickness, as shown in **Fig. 5H**. These results suggest that MET treatment may prevent atherosclerosis in obese and diabetic rats.

### **11. Histopathological assessment of heart on the effect of MET in the progression of cardiac structure defects in insulin-resistant and diabetic rats**

Finally, we studied the histological changes in the heart tissues of our experimental animals (**Fig. 6**). In the obese rats, we observed multifocal myocardial degeneration and the formation of multifocal fat vacuoles in the cardiomyocytes. Additionally, we noted the infiltration of MNCs and vascular degeneration in the myocardium of these obese rats (**Fig. 6B**). In contrast, the group treated with MET exhibited less myocardial degeneration and only mild fat vacuole formation (**Fig. 6C**).

The diabetic rats exhibited moderate to severe myocardial degeneration, the formation of necrosis, and multifocal hypertrophy in myocytes. Numerous vacuoles were observed in the myocardium, accompanied by accumulated MNC infiltrations (**Fig. 6E**). The group treated with MET (HFD + STZ + MET) demonstrated a reduction in myocardial degeneration, necrosis, MNC infiltration, vacuoles, and myocyte hypertrophy (**Fig. 6F**). These results confirm that MET treatment mitigated cardiac hypertrophy and the degeneration of cardiomyocytes.

## **DISCUSSION**

In the present study, we demonstrated the following main findings:

1. For the first time, we observed and documented a significant reduction in Sestrin2 expression in the aorta and heart tissues of obese and diabetic rats. Additionally, we noted a significant change in the activation of AMPK and mTORC1 in the aorta and heart tissues under obese and diabetic conditions.
2. Alterations were observed in the expression of pro-inflammatory adhesion molecules and matrix metalloproteinases, which are the key processes involved in atherogenesis.
3. Another innovative discovery is that MET treatment reinstated the expression levels of Sestrin2 in both the aorta and heart of the obese and diabetic model. This consequently reduced the atherogenic events triggered by dyslipidaemic and hyperglycaemic conditions.

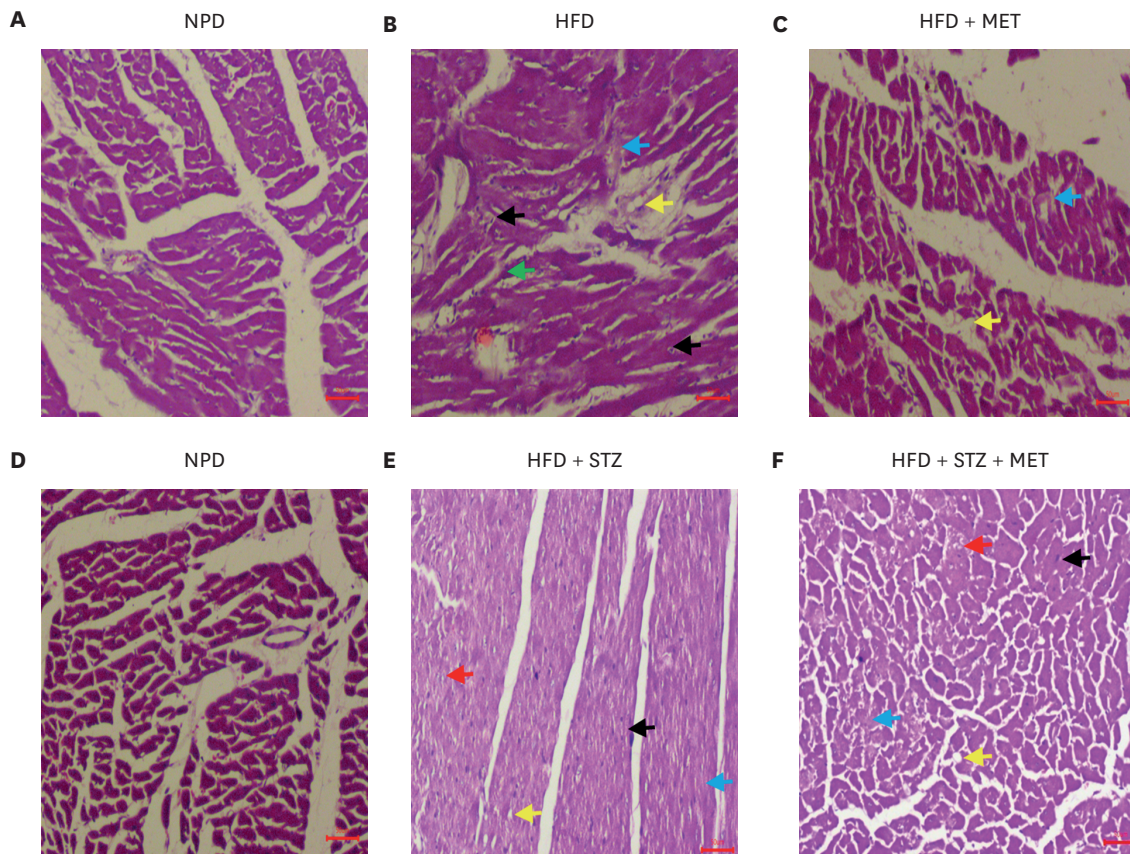


**Fig. 6.** Histological examination of cardiac tissue: (A, D) NPD rats show normal histopathology of the heart (B) HFD rats show myocardial degeneration (light blue arrow), fat vacuoles (yellow arrow), mononuclear cells infiltration (black arrow), vascular degeneration in myocardium (green arrow). (C) HFD+MET rats show reduced myocardial degeneration, mild fat vacuoles. (D) HFD + STZ rats show myocardial degeneration, fat vacuoles, mononuclear cells infiltration, vascular degeneration, necrosis formation (red arrow), and hypertrophy in the myocardium (dark blue arrow). (E) HFD + STZ + MET rats show decreased myocardial degeneration, necrosis, mononuclear cell filtration, vacuoles, and hypertrophy in myocytes (histological structure analysis using haematoxylin and eosin staining, scale bar:  $\times 10=50\ \mu\text{m}$ ).

NPD, normal-pellet diet; HFD, high-fat diet; MET, metformin; STZ, streptozotocin.

Although numerous clinical trials have shown that MET can reduce CVD outcomes and cardiac defects,<sup>11</sup> the precise protective role of MET in relation to CVD and atherosclerosis remains unclear. Therefore, we investigated the impact of MET on atherogenicity under conditions of obesity and diabetes. A prior study reported that MET can decrease body weight and BMI.<sup>12</sup> Consistent with this, our study also found that MET treatment reduced the body weight of obese rats. Additionally, we observed the expected glucose-lowering effect of MET in diabetic rats. Under diabetic conditions, the loss of insulin action in adipocytes and the liver increases the production of LDL-C, VLDL-C, and triglycerides, even when glycogen storage is sufficient.<sup>13</sup> This could explain the altered lipid profile in diabetes-induced animal models, as observed in our study.

Previous studies have shown that MET can reduce levels of total cholesterol, LDL-C, VLDL-C, and triglycerides.<sup>14</sup> MET is known to decrease postprandial lipemia through the activation of AMPK, which in turn suppresses fatty acid desaturases by promoting insulin sensitivity. In our research, we discovered that animals treated with MET exhibited lower plasma levels of cholesterol, triglycerides, VLDL-C, and the CHO/HDL-C ratio compared to obese (HFD) and diabetic (HFD+STZ) rats. Additionally, we found that MET treatment reduced plasma atherogenicity in both obese and diabetic models. This aligns with a prospective study by

Kashi et al.<sup>15</sup>, which reported that treatment with MET decreased the plasma atherogenic index in type2 diabetes.

It is well known that MET plays a role in activating AMPK, which acts as a fuel gauge and energy sensor within cells.<sup>16,17</sup> AMPK regulates the development of vascular dysfunction by preventing the macrophage activation and inhibiting the secretion of pro-inflammatory cytokines, and other atherogenic processes.<sup>18</sup> In our study, we observed changes in the activity of AMPK and mTOR under diabetic and obese conditions. However, treatment with MET restored the normal activities of these two enzymes.

Sestrin2 is known to be a metabolic regulator that modulates the AMPK-mTORC pathway under various stress conditions. In our previous research, we discovered that Sestrin2 played a role in regulating the primary events of atherogenesis progression.<sup>6</sup> Likewise, in this study, we observed a decrease in Sestrin2 expression levels in both the aorta and heart tissues of obese and diabetic rats. However, treatment with MET restored these levels in both tissues. These results underscore the potential protective role of MET, which may function through the upregulation of Sestrin2 by AMPK.

Our study found a significant increase in pro-inflammatory markers (M1 markers) in the aorta and heart tissues of obese and diabetic rats (HFD and HFD+STZ group). This confirms the role of inflammation in the progression of atherogenesis. In our previous study, we also observed an increase in pro-inflammatory markers in THP1 cells subjected to glucolipototoxicity.<sup>6</sup> MET decreased all these abnormalities, demonstrating its ability to regulate monocyte polarization through the Sestrin2-mTOR pathway. Additionally, we observed an increase in M2 markers (anti-inflammatory phenotype) following MET treatment.

Monocyte adherence to endothelial cells is the basis for atherosclerosis development. The transmigration and adhesion of monocytes into the sub-endothelial space, in response to stimuli, play a crucial role in the development of early atherosclerotic lesions and enhance disease progression in later stages.<sup>19</sup> In our study, we observed a significant increase in the expression of adhesion molecules in the aorta and heart tissues of rats on a HFD and HFD combined with STZ (HFD + STZ). MET mitigated the impact of HFD and HFD + STZ on the expression of these adhesion molecules. The formation of foam cells represents the subsequent stage in the progression of atherosclerotic plaques. Macrophage derived foam cell formation is a predominant step in the process of arterial atherosclerotic plaque formation. In our histological studies, we noted numerous foam cells (vacuoles) in the tunica media and tunica intima of the aorta in HFD + STZ rats. These foam cells were significantly fewer in the rats treated with MET. Our findings indicate that both obesity and diabetes stimulate the expression of adhesion molecules and the formation of foam cells in the tissues of the aorta and heart, leading to the atherosclerotic process. This process can be prevented and minimized with MET treatment.

In the later stages of disease progression, plaques can develop a stable fibrous cap that isolates them from the surrounding vessel environment. The destabilization of these plaques happens through the depletion and rupture of the fibrous cap, a process facilitated by matrix metalloproteinases that trigger the degradation of the extracellular matrix. In our research, we discovered a significant increase in these matrix metalloproteinases in the aorta and heart of animals treated with both an HFD and a combination of HFD and STZ which contributes to the accumulation of plaques. Prior studies have reported that inhibiting mTORC1 can

reduce matrix accumulation and fibrous formation in the aorta.<sup>20</sup> Similarly, we found that MET treatment decreased the activation of both MMP2 and MMP9. Additionally, MET treatment in HFD and HFD+STZ rats led to an upregulation of TIMP-1, a regulatory factor of these enzymes.

We also found that MET treatment reduced the thickness of the tunica intima and tunica media in aortic tissue. Prior research has shown that MET treatment can lessen the severity of atherosclerotic lesions in diabetic models.<sup>21,22</sup> Additionally, we observed that MET treatment diminished fiber disorganization reduced the number of foam cell vacuoles, and decreased cell fragmentation in the aorta. These findings suggest that MET may play a preventative role in the progression of atherosclerosis in diabetic rats.

The enlargement of the heart, as seen in the HFD and HFD + STZ models, signifies hypertrophy. Additionally, degeneration, necrosis, and cellular hypertrophy were noted in the cardiomyocytes of animals treated with HFD and HFD + STZ. This indicates cardiac cell damage and remodelling in conditions of obesity and diabetes. The administration of MET significantly reversed the tissue damage induced by HFD and STZ treatment.

In our study, we treated obese and diabetic rats with MET for a period of 14 weeks. This approach could potentially simulate the long-term pathophysiological conditions found in humans. Therefore, our findings illustrate the enduring impact of MET in averting atherosclerotic events.

In summary, our preclinical study has shown that MET treatment enhances the expression of Sestrin2 and decreases mTOR activation, which in turn reduces both the atherogenic process and cardiac remodelling. Our research provides a mechanistic demonstration that MET impedes the progression of atherogenesis and cardiac damage/hypertrophy through the coordinated regulation of the Sestrin2-AMPK-mTORC1 axis signalling. Furthermore, our study underscores the potential of Sestrin2 as an emerging novel drug target for atherogenesis in obese and diabetic conditions. Looking ahead, modifications to the Sestrin2 gene and the atherosclerotic model could shed more light on the role of Sestrin2 in the regulation of atherogenesis under metabolic syndrome.

## **ACKNOWLEDGEMENTS**

We thank Dr. Pazhanivel, N. Professor, Department of Veterinary Pathology, Madras Veterinary College, Chennai for his help in histopathological assessment. Mr. Prabhu Durairaj, animal house technician is greatly acknowledged for his help in the maintenance and handling of animals.

## **SUPPLEMENTARY MATERIALS**

### **Supplementary Table 1**

Primer sequences

[Click here to view](#)

**Supplementary Table 2**

Clinical and biochemical characterization of obesity and diabetic rats

[Click here to view](#)

**Supplementary Fig. 1**

Experimental design.

[Click here to view](#)

**Supplementary Fig. 2**

(A) body weight at 45<sup>th</sup> day. (B) Plasma cholesterol at 45<sup>th</sup> day. (C) Plasma triglycerides at 45<sup>th</sup> day. (D) Plasma HDL-C at 45<sup>th</sup> day. (E) Cholesterol and HDL-C ratio. All values are represented as mean  $\pm$  SEM.

[Click here to view](#)

**Supplementary Fig. 3**

(A) ITT as represented by glucose disposal after insulin challenge during 0 to 90 minutes. (B) AUC 0–90 minutes after insulin administration. All values are represented as mean $\pm$ SEM. (C) OGTT as represented by glucose levels during 0–120 minutes. (D) AUC 0–120 minutes after glucose challenge. All values are represented as mean  $\pm$  SEM.

[Click here to view](#)

**REFERENCES**

1. Cornier MA, Dabelea D, Hernandez TL, Lindstrom RC, Steig AJ, Stob NR, et al. The metabolic syndrome. *Endocr Rev* 2008;29:777-822.  
[PUBMED](#) | [CROSSREF](#)
2. Kassi E, Pervanidou P, Kaltsas G, Chrousos G. Metabolic syndrome: definitions and controversies. *BMC Med* 2011;9:48.  
[PUBMED](#) | [CROSSREF](#)
3. World Health Organization. Obesity and overweight [Internet]. Geneva: World Health Organization [cited 2023 Jun 9]. 2021. Available from: <https://www.who.int/news-room/fact-sheets/detail/obesity-and-overweight>.
4. Katakami N. Mechanism of development of atherosclerosis and cardiovascular disease in diabetes mellitus. *J Atheroscler Thromb* 2018;25:27-39.  
[PUBMED](#) | [CROSSREF](#)
5. Libby P, Buring JE, Badimon L, Hansson GK, Deanfield J, Bittencourt MS, et al. Atherosclerosis. *Nat Rev Dis Primers* 2019;5:56.  
[PUBMED](#) | [CROSSREF](#)
6. Sundararajan S, Jayachandran I, Balasubramanyam M, Mohan V, Venkatesan B, Manickam N. Sestrin2 regulates monocyte activation through AMPK-mTOR nexus under high-glucose and dyslipidemic conditions. *J Cell Biochem* 2019;120:8201-8213.  
[PUBMED](#) | [CROSSREF](#)
7. Sundararajan S, Jayachandran I, Subramanian SC, Anjana RM, Balasubramanyam M, Mohan V, et al. Decreased Sestrin levels in patients with type 2 diabetes and dyslipidemia and their association with the severity of atherogenic index. *J Endocrinol Invest* 2021;44:1395-1405.  
[PUBMED](#) | [CROSSREF](#)
8. Luo F, Das A, Chen J, Wu P, Li X, Fang Z. Metformin in patients with and without diabetes: a paradigm shift in cardiovascular disease management. *Cardiovasc Diabetol* 2019;18:54.  
[PUBMED](#) | [CROSSREF](#)



9. Zhou G, Myers R, Li Y, Chen Y, Shen X, Fenyk-Melody J, et al. Role of AMP-activated protein kinase in mechanism of metformin action. *J Clin Invest* 2001;108:1167-1174.  
[PUBMED](#) | [CROSSREF](#)
10. Balakumar M, Prabhu D, Sathishkumar C, Prabu P, Rokana N, Kumar R, et al. Improvement in glucose tolerance and insulin sensitivity by probiotic strains of Indian gut origin in high-fat diet-fed C57BL/6J mice. *Eur J Nutr* 2018;57:279-295.  
[PUBMED](#) | [CROSSREF](#)
11. Holman RR, Paul SK, Bethel MA, Matthews DR, Neil HA. 10-year follow-up of intensive glucose control in type 2 diabetes. *N Engl J Med* 2008;359:1577-1589.  
[PUBMED](#) | [CROSSREF](#)
12. Yanovski JA, Krakoff J, Salaita CG, McDuffie JR, Kozlosky M, Sebring NG, et al. Effects of metformin on body weight and body composition in obese insulin-resistant children: a randomized clinical trial. *Diabetes* 2011;60:477-485.  
[PUBMED](#) | [CROSSREF](#)
13. Ormazabal V, Nair S, Elfeky O, Aguayo C, Salomon C, Zuñiga FA. Association between insulin resistance and the development of cardiovascular disease. *Cardiovasc Diabetol* 2018;17:122.  
[PUBMED](#) | [CROSSREF](#)
14. Lin SH, Cheng PC, Tu ST, Hsu SR, Cheng YC, Liu YH. Effect of metformin monotherapy on serum lipid profile in statin-naïve individuals with newly diagnosed type 2 diabetes mellitus: a cohort study. *PeerJ* 2018;6:e4578.  
[PUBMED](#) | [CROSSREF](#)
15. Kashi Z, Mahrooz A, Kianmehr A, Alizadeh A. The role of metformin response in lipid metabolism in patients with recent-onset type 2 diabetes: HbA1c level as a criterion for designating patients as responders or nonresponders to metformin. *PLoS One* 2016;11:e0151543.  
[PUBMED](#) | [CROSSREF](#)
16. Zang M, Zuccollo A, Hou X, Nagata D, Walsh K, Herscovitz H, et al. AMP-activated protein kinase is required for the lipid-lowering effect of metformin in insulin-resistant human HepG2 cells. *J Biol Chem* 2004;279:47898-47905.  
[PUBMED](#) | [CROSSREF](#)
17. Li J, Benashski SE, Venna VR, McCullough LD. Effects of metformin in experimental stroke. *Stroke* 2010;41:2645-2652.  
[PUBMED](#) | [CROSSREF](#)
18. Srivastava RA, Pinkosky SL, Filippov S, Hanselman JC, Cramer CT, Newton RS. AMP-activated protein kinase: an emerging drug target to regulate imbalances in lipid and carbohydrate metabolism to treat cardio-metabolic diseases. *J Lipid Res* 2012;53:2490-2514.  
[PUBMED](#) | [CROSSREF](#)
19. Schwartz CJ, Valente AJ, Sprague EA, Kelley JL, Cayatte AJ, Mowery J. Atherosclerosis. Potential targets for stabilization and regression. *Circulation* 1992.86 Suppl:III117-III123.  
[PUBMED](#)
20. Jiao Y, Li G, Li Q, Ali R, Qin L, Li W, et al. mTOR (Mechanistic Target of Rapamycin) inhibition decreases mechanosignaling, collagen accumulation, and stiffening of the thoracic aorta in elastin-deficient mice. *Arterioscler Thromb Vasc Biol* 2017;37:1657-1666.  
[PUBMED](#) | [CROSSREF](#)
21. Asai A, Shuto Y, Nagao M, Kawahara M, Miyazawa T, Sugihara H, et al. Metformin attenuates early-stage atherosclerosis in mildly hyperglycemic oikawa-nagao mice. *J Atheroscler Thromb* 2019;26:1075-1083.  
[PUBMED](#) | [CROSSREF](#)
22. Wang Q, Zhang M, Torres G, Wu S, Ouyang C, Xie Z, et al. Metformin suppresses diabetes-accelerated atherosclerosis via the inhibition of Drp1-mediated mitochondrial fission. *Diabetes* 2017;66:193-205.  
[PUBMED](#) | [CROSSREF](#)